Journal of Magnetic Resonance 204 (2010) 139–144

Contents lists available at ScienceDirect

Journal of Magnetic Resonance

journal homepage: www.elsevier.com/locate/jmr

Magnetic field-cycling NMR and ^{14}N, ^{17}O quadrupole resonance in the explosive pentaerythritol tetranitrate (PETN) ☆

John A.S. Smith [a], Timothy J. Rayner [c], Michael D. Rowe [a,*], Jamie Barras [a], Neil F. Peirson [b], Andrew D. Stevens [a], Kaspar Althoefer [a]

[a] Department of Mechanical Engineering, King's College London, Strand, London WC2R 2LS, UK
[b] Centenary, Ropery Road, Gainsborough, Linconshire DN21 2PD, UK
[c] Tronning, Grange Road, Crawley Down, West Sussex RH10 4JT, UK

ARTICLE INFO

Article history:
Received 5 January 2010
Revised 18 February 2010
Available online 21 February 2010

Keywords:
PETN
Magnetic field-cycling NMR
T_1 dispersion
Quadrupole dips
^{14}N and ^{17}O NQR

ABSTRACT

The explosive pentaerythritol tetranitrate (PETN) $C(CH_2–O–NO_2)_4$ has been studied by ^1H NMR and ^{14}N NQR. The ^{14}N NQR frequency and spin–lattice relaxation time T_{1Q} for the ν_+ line have been measured at temperatures from 255 to 325 K. The ^1H NMR spin–lattice relaxation time T_1 has been measured at frequencies from 1.8 kHz to 40 MHz and at temperatures from 250 to 390 K. The observed variations are interpreted as due to hindered rotation of the NO_2 group about the bond to the oxygen atom of the CH_2–O group, which produces a transient change in the dipolar coupling of the CH_2 protons, generating a step in the ^1H T_1 at frequencies between 2 and 100 kHz. The same mechanism could also explain the two minima observed in the temperature variation of the ^{14}N NQR T_{1Q} near 284 and 316 K, due in this case to the transient change in the $^{14}N\ldots{}^1H$ dipolar interaction, the first attributed to hindered rotation of the NO_2 group and the second to an increase in torsional amplitude of the NO_2 group due to molecular distortion of the flexible CH_2–O–NO_2 chain which produces a 15% increase in the oscillational amplitude of the CH_2 group. The correlation times governing the ^1H T_1 values are approximately 25 times longer than those governing the ^{14}N NQR T_{1Q}, explained by the slow spin–lattice cross-coupling between the two spin systems. At higher frequencies, the ^1H T_1 dispersion results show well-resolved dips between 200 and 904 kHz assigned to level crossing with ^{14}N and weaker features between 3 and 5 MHz tentatively assigned to level crossing with ^{17}O.

1. Introduction

Magnetic field-cycling methods can be used to measure T_1 dispersion (the variation of the NMR spin–lattice relaxation time T_1 with magnetic field [1–3]). Magnetic fields can be switched on and off in times of a millisecond [1,4] enabling T_1 values as short as a few ms to be measured in very low magnetic fields [1,4]. In addition, quadrupole interactions can be studied by the phenomenon of quadrupole dips [5]. This paper presents such a study of the explosive pentaerythritol tetranitrate (PETN) $C(CH_2–O–NO_2)_4$, in which quadrupole dips from ^{14}N and possibly ^{17}O (in natural abundance) have been detected. The temperature dependence of the zero-field ^{14}N NQR frequencies and T_{1Q} relaxation times has also been measured to compare with these results. The molecular structure of PETN is shown in Fig. 1.

2. Experimental methods

The T_1 dispersion measurements were conducted between ^1H NMR frequencies of 1.8 kHz to 15 MHz on a fast field-cycling NMR spectrometer with a maximum magnetic field of 1 T and a field stability of 1 part in 10^5, which could be switched in 0.7 ms, with a settling time of between 2 and 4 ms depending on the field value [4]. The high field (42 MHz) NMR coil was a solenoid consisting of eight turns of copper wire wound on a former of 10 mm diameter and 10 mm length, across which the field homogeneity was close to two parts in 10^5. The samples consisted of 2 g of, the room temperature stable, phase I [6,7] PETN mixed with a small amount of additive. T_1 values of between 1 ms and 100 s were measured by standard inversion recovery methods [8] using multiple-pulse sequences with signal averaging to improve signal-to-noise ratio. The measurements were conducted over a range of temperatures between 250 and 370 K to include the region of

☆ This work was funded in part by the UK Defense Science and Technology Laboratory (DSTL Fort Halstead).

* Corresponding author. Fax: +44 20 7848 2699.
E-mail addresses: john.smith@kcl.ac.uk (J.A.S. Smith), TRayner@rapiscansystems.com (T.J. Rayner), michael.d.rowe@kcl.ac.uk (M.D. Rowe), jamie.barras@kcl.ac.uk (J. Barras), nqr2004@yahoo.co.uk (N.F. Peirson), andrewstevens13@tiscali.co.uk (A.D. Stevens), k.althoefer@kcl.ac.uk (K. Althoefer).

1090-7807/$ - see front matter © 2010 Elsevier Inc. All rights reserved.
doi:10.1016/j.jmr.2010.02.019

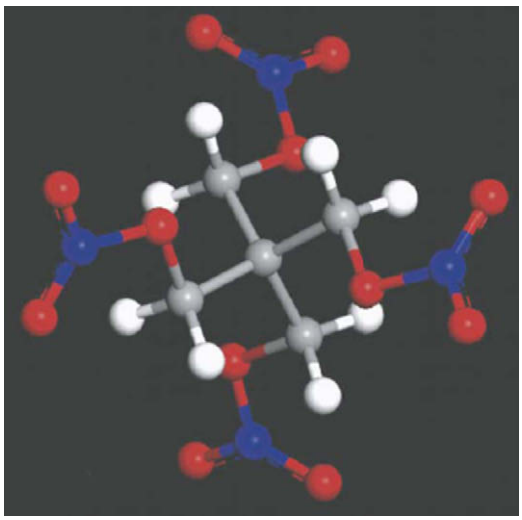

Fig. 1. Molecular structure of pentaerythritol tetranitrate (PETN) reproduced from J. Crystal Growth 292 (2006) 461–467 by kind permission of Dr. Luis A. Zepeda-Ruiz. The carbon, hydrogen, oxygen and nitrogen atoms are coloured grey, white, red and blue, respectively. (For interpretation of color mentioned in this figure the reader is referred to the web version of the article.)

interest in NQR detection methods for this explosive, but some fixed-field NMR measurements were also undertaken with the same samples at 15 and 40 MHz at temperatures of up to 390 K, and 26 K below the melting point, the maximum attainable before significant thermal decomposition began. The observed 40 MHz ^{1}H NMR spectrum (Fig. 2) showed two components with different line-widths, a narrow component (B) with short T_1 values, typically 0.1 s and assigned to the additives, and a broad doublet (A) with long T_1 values of 100 s or more assigned to the NMR spectrum of the CH_2 groups in PETN with a dipolar splitting close to 25 kHz, corresponding to an interproton distance of 171 pm. The influence of the short T_1 component was removed by means of a T_1 filter for which all points of the relaxation data before 0.1 s were rejected.

Pulsed ^{14}N quadrupole resonance measurements were conducted on a Tecmag "Libra" RF spectrometer. Line frequencies and spin–lattice relaxation times T_{1Q} were measured over a temperature range from 283 to 323 K. Multiple-pulse echo sequences [9] were used for signal enhancement and the saturation recovery method [8] was used to obtain the T_{1Q} values assuming a single relaxation time. The sample was 140 g of Detasheet (63% PETN) and the temperature was controlled by circulating silicone oil from a thermostated oil bath round the sample. The temperature range was limited to reduce risks in handling this quite large sample of explosive.

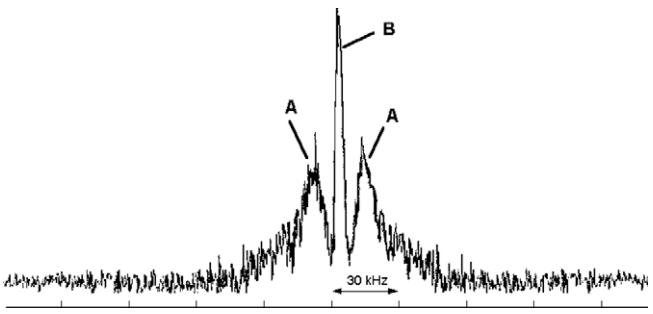

Fig. 2. A 40 MHz ^{1}H NMR spectrum of solid PETN at 300 K showing the two components with different line-widths (scale in units of 30 kHz).

3. Results and discussion

3.1. The temperature variation of the ^{14}N NQR ν_+ line frequency

^{14}N quadrupole resonance frequencies are already known for PETN at ambient temperatures, with $\nu_+ = 890$ and $\nu_- = 495$ kHz [10]. Only one set of ^{14}N NQR frequencies is observed as predicted by the symmetry of the molecules in the crystal, which sit on four-fold inversion axes [6,7]. We have measured the temperature variation of ν_+ line frequency, and the results are plotted in Fig. 3.

The temperature variation has two approximately linear regions indicated by the two linear fits in Fig. 3. The first from 258 to 296 K gives a frequency temperature coefficient of –90.1 [Hz] [K^{-1}] and the second from 296 to 323 K gives a higher value of –117.6 [Hz] [K^{-1}]. It is difficult to identify the exact point of transition from one region to the other but it lies between 296 and 306 K. The errors in the temperature are estimated to be ±0.25 K and in the frequency ±0.1 kHz. A major contribution to this temperature dependence is expected to come from the torsional oscillation of the NO_2 group about the bond to the oxygen atom of the CH_2–O group, which at constant volume should follow the Bayer–Kushida equation [11].

$$\nu(T) = \nu(0) - (3\hbar\nu_0/2)\sum_i \frac{A_i}{\omega_i}\left(\frac{1}{\exp(\hbar\omega_i/kT)-1}\right) \quad (1)$$

where the zero temperature term $\nu(0)$ is given by:

$$\nu(0) = \nu_0\left[1 - (3/4)\hbar\sum_i A_i/\omega_i\right]$$

ω_i is the torsional oscillation frequency of the ith mode, $\nu(T)$ is the NQR line frequency at a temperature T, and ν_0 the resonance frequency in a fictitious "static" lattice. A_i consists of two terms. The first is due to the averaging of the electric field gradient at the nuclear site by the torsional oscillations, for which $A_i = 1/I_i$, I_i being the corresponding moment of inertia, and the second is due to molecular distortion. The temperature variation of both linear regions in Fig. 3 could be expressed by extracting the linear term in Eq. (1) to give for one torsional mode:

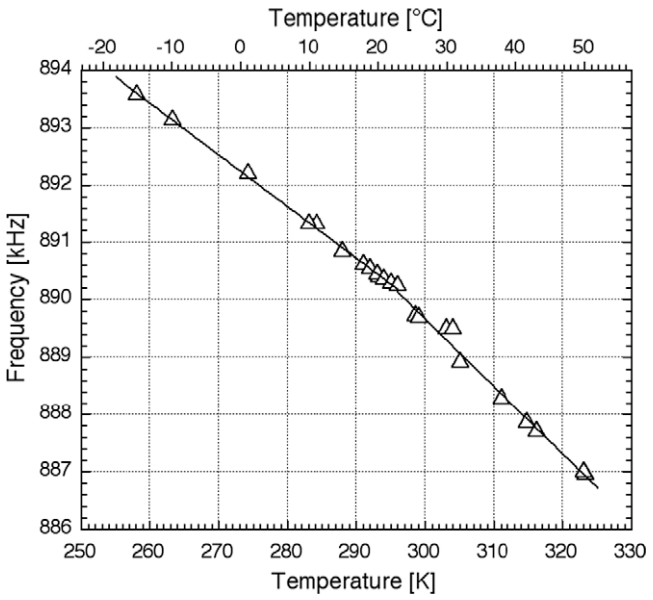

Fig. 3. Temperature variation of the 14 N NQR ν_+ line frequency for PETN between 258 and 323 K.

$$v(T) = v_0 - \frac{3v_0}{2I_t(\omega_t)^2} \cdot kT \quad (2)$$

Assuming that the difference in slope above and below about 296 K is due entirely to a change in the torsional oscillation frequency of the NO_2 group, it corresponds to a 25% decrease in ω_i. Assuming a value for I_i of 64.6×10^{-47} kg m^2 calculated from bond lengths and angles for the NO_2 group taken from the crystal structure [5], we predict a torsional frequency of 83 cm^{-1} above 300 K and 95 cm^{-1} below, which may be compared with values for C–NO_2 torsional frequencies of 106–115 cm^{-1} in *m*-chloronitrobenzene [12] and 21 cm^{-1} in 3-nitrobenzene sulphonyl chloride [13]. Torsional frequencies are known to be temperature dependent, often decreasing linearly with increase of temperature [14], but the behaviour observed in PETN is more unusual, since the change occurs over a small temperature range. For a simple harmonic oscillator, the change in torsional frequency implies an increase in the root mean square amplitude of oscillation by a factor of approximately 7%. We propose that this is due to the onset of hindered rotation of the NO_2 group about the bond to the oxygen atom of the CH_2–O group, to be discussed in the next section, which produces a molecular distortion of the flexible CH_2–O–NO_2 group in such a way as to reduce the torsional frequency and so increase the rms oscillational amplitude.

3.2. ^1H T_1 dispersion measurements

Field-cycling experiments were conducted at sample temperatures between 274 and 366 K and magnetic fields (in units of the ^{1}H NMR frequency) between 1.8 kHz and 15 MHz. It is assumed that there will be no level-crossing effects because of the fast rate of change of the magnetic field of 1400 T s^{-1}. A typical plot over the whole field range at 330 K is shown in Fig. 4, there are three particular regions of interest and we will deal with the detail of each of these separately. The first region between 2 and 110 kHz, shows a step in T_1, the second between 150 kHz and 1 MHz, has at least six quadrupole dips (see Fig. 6) and the third between 1 and 15 MHz has two broad, shallow dips between 2.2 and 5 MHz which we tentatively assign to level crossing with ^{17}O.

Plots of $1/T_1$ for the first low field region at different temperatures are shown in Fig. 5. If plots of $\ln T_1$ against T^{-1} from the results in Fig. 5 at fixed fields of 1.8 and 70 kHz are fitted to the equation.

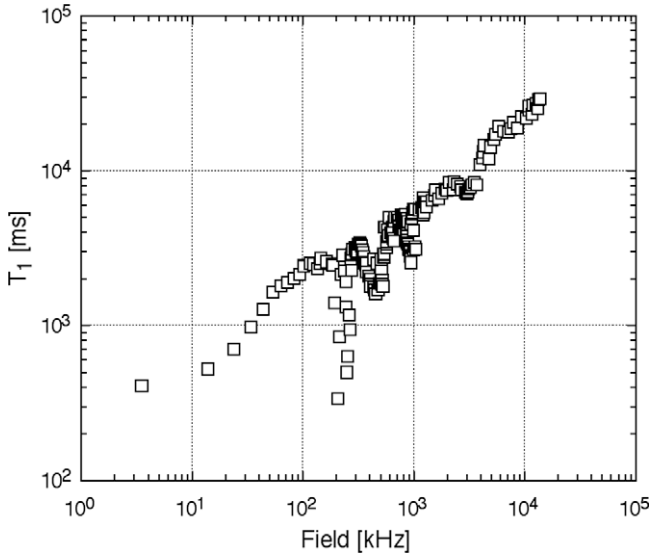

Fig. 4. ^{1}H T_1 dispersion in PETN at 330 K over the full field range up to 15 MHz.

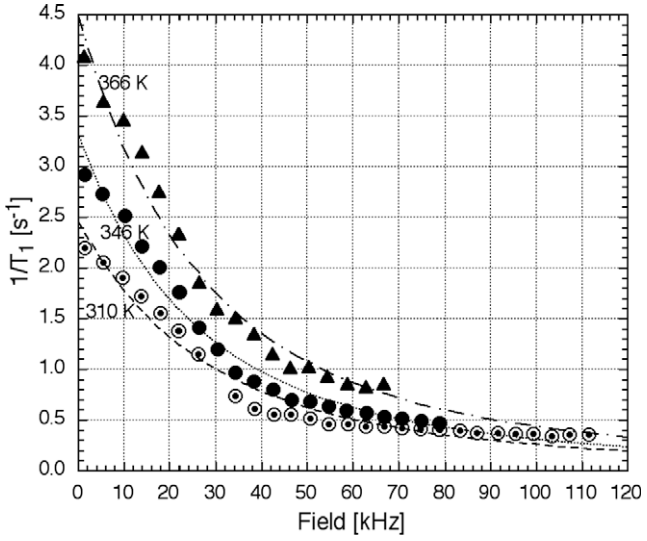

Fig. 5. Plots of $1/T_1$ versus ^{1}H NMR frequency from low field ^{1}H T_1 dispersion measurements on PETN between 1.8 and 110 kHz at the three temperatures 366, 346 and 310 K, together with calculated fits.

$$\frac{1}{T_1} = Ae^{E_a/RT} \quad (3)$$

the activation energies E_a deduced are 9.2 kJ mol^{-1} at the former and 10.7 kJ mol^{-1} at the latter, equal within experimental error. We suggest that the relaxation mechanism is the small transient rotation of the CH_2 group which accompanies the hindered rotation of the NO_2 group and which also modulates the ^{14}N…^{1}H dipolar interaction. We therefore fit the data of Fig. 5 using Eq. (4), previously used to analyse a similar (but larger) reorientation of the interproton vector of the two hydrogen-bonded protons in the dimer of *p*-toluic acid – d_7 [15]. However, here we assume that the probability of the occupation of the two sites is equal and we have included a term for the local dipolar field which is significant when the applied field is low.

$$\left[\frac{1}{T_1}\right] = C\left(\frac{\tau_c}{1+((\omega_H+\omega_L)\tau_c)^2} + \frac{4\tau_c}{1+4((\omega_H+\omega_L)\tau_c)^2}\right) \quad (4)$$

with

$$C = \frac{3}{80}\gamma_H^4 h^2 \left(\frac{\mu_0}{4\pi}\right)^2 \frac{\sin^2(2\alpha_{HH})}{r_{HH}^6} \quad (5)$$

and

$$\tau_c = \tau_0 e^{(E_a/RT)} \quad (6)$$

where $2\alpha_{HH}$ is the mean change in the angular orientation of the interproton vector of the CH_2 group, r_{HH} the interproton distance within this group (assumed to equal 171 pm), γ_H is the proton gyromagnetic ratio and $\omega_H = 2\pi\nu_H$ and $\omega_L = 2\pi\nu_L$, where ν_H and ν_L are the ^{1}H NMR frequencies in the applied magnetic field and in the local dipolar (25 kHz) field, respectively.

The fits shown in Fig. 5 to the $1/T_1$ plots for the three temperatures 310, 346 and 366 K were all obtained with $E_a = 10.5$ kJ mol^{-1} and gave the temperature dependent values of τ_0 and C presented in Table 1 together with the resulting values of τ_c and $2\alpha_{HH}$. The values of the latter are too small to produce any significant effect in the dipolar splitting observed in the ^{1}H NMR spectrum of Fig. 2. The expected low field plateau has not been reached in these measurements, although there is some evidence for it in Fig. 4. This may be because of the large dipolar term; nevertheless the fits should not be regarded as unique. The use of the fixed value of

Table 1
Parameters of Eqs. (4)–(6) obtained from the fits of Fig. 5.

T [K]	C [s^{-2}]	τ_0 [μs]	τ_c [μs]	$2\alpha_{HH}$ [°]
310	2.8×10^5	0.053	3.14	3.3
346	3.7×10^5	0.092	3.55	3.8
366	5.0×10^5	0.108	3.40	4.4

E_a = 10.5 kJ mol^{-1} is a compromise, it is in good agreement with the values mentioned above as well as the value found in Section 3.3 and also gives reasonable fits for all three temperatures. However, this also requires C and τ_0 to be temperature dependent and here we assume this could be a consequence of the flexibility of the CH_2–O–NO_2 chain which is only fixed at one end, as mentioned in Section 3.1.

The second region of the proton T_1 dispersion from 150 kHz to 1 MHz contains six quadrupole dips which have been assigned to the three ^{14}N NQR frequencies, for which ν_+ and ν_- are close to those observed in zero-field pulsed NQR, together with the corresponding double proton relaxation jumps [16]. Fig. 6 shows the detail for this region taken from two separate measurements with PETN at a temperature of 330 K; the dips are assigned as in Table 2.

The dips have been fitted to Eq. (7):

$$\frac{1}{T_1} = R_a + R_b \tag{7}$$

in which R_a refers to the expected contribution in the absence of the dips and R_b to that of the dips themselves [17]. We assume that the former can be described by a simple power law of the form:

$$R_a = A\omega_H^{-a} \tag{8}$$

and the latter by a Lorentzian function of the form:

$$R_b = \sum B^{(j)} 2\tau_{NH}/(1 + (\omega_Q^{(j)} - \omega_H)^2 \tau_{NH}^2) \tag{9}$$

where the summation is over the index j representing the six quadrupole dip frequencies given in Table 2. The parameter τ_{NH} is a measure of the spin–lattice cross-coupling time between the ^{14}N and ^{1}H spin systems at level crossing and the width of each dip is given by $1/\pi\tau_{NH}$. Fig. 6 shows a fit to T_1 data using Eqs. (8) and (9) in which different values of $B^{(j)}$ were assumed for each dip along with two different values of τ_{NH}, depending on whether the dip corresponds

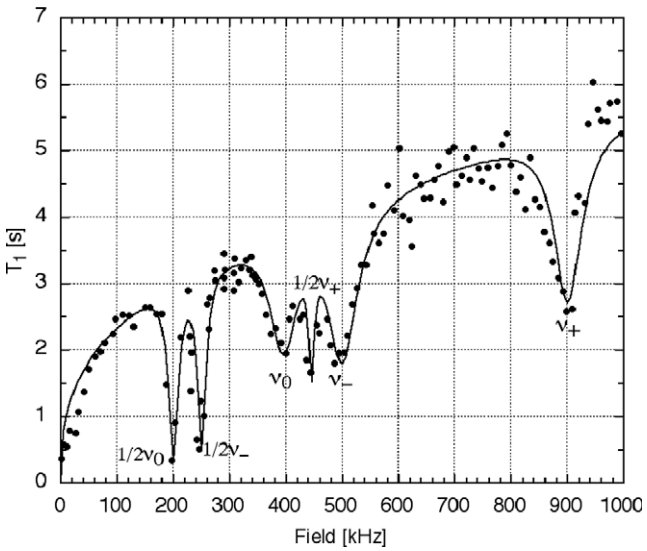

Fig. 6. ^{1}H T_1 dispersion in PETN at 330 K from 1.8 kHz to 1 MHz taken from two separate experiments with a calculated fit.

Table 2
Dip frequencies and assignments for PETN.

Dip assignment	Dip frequency (kHz)
$\frac{1}{2}\nu_0$	200
$\frac{1}{2}\nu_-$	250
$\frac{1}{2}\nu_+$	445
ν_0	395
ν_-	499
ν_+	904

to a single proton or double proton jump. The fit gave τ_{NH} = 43.4 μs for the former and τ_{NH} = 7.6 μs for the latter together with a value of a = 0.37 in the power term R_a.

3.3. The temperature variation of ^{1}H T_1 at fixed NMR fields

Fig. 7 shows the temperature variation of the proton T_1 at 40 MHz for PETN between 217 and 380 K from measurements obtained using two PETN samples taken from different batches of the explosive, the most notable feature is a broad and rather shallow minimum of 110 s between 280 and 310 K. Similar results were obtained at 15 MHz with a T_1 minimum of 65 s also close to 280 K. Fig. 7 also shows a fit, again using Eqs. (4)–(6), with the following parameter values:

$$C = 1.58 \times 10^6 \quad \tau_0 = 0.027 \text{ ns} \quad E_a = 11.1 \text{ kJ mol}^{-1}$$

the latter being in good agreement with the values of obtained from the T_1 dispersion in Section 3.2. The value of C obtained here is significantly higher and that of τ_0 lower than the three temperature dependent values obtained in Section 3.2, given in Table 1, but this was the only way we could fit the much higher field data of Fig. 7. We do not have a functional form for the temperature dependence of C to use in this fit but anyway this would be unlikely to result in values of C in agreement with Table 1.

According to Eq. (4), the ratio of the minimum T_1 values at 40 and 15 MHz should be 1.86 compared to the observed value of 1.69, the discrepancy being presumably due to approximations made in the analysis.

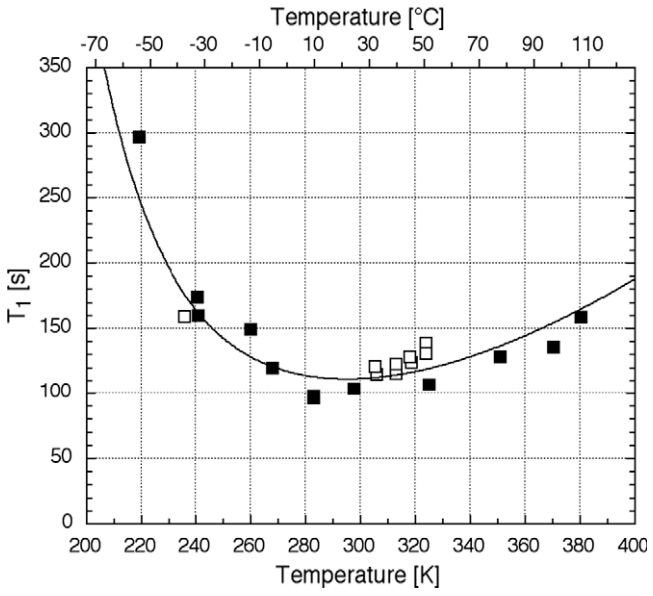

Fig. 7. Temperature variation of the ^{1}H T_1 in PETN at 40 MHz between 217 and 380 from measurements obtained using two PETN samples taken from different batches of the explosive indicated by the two different symbols.

3.4. The temperature variation of the ^{14}N NQR ν_+ line spin–lattice relaxation time T_{1Q}

This shows unusual behaviour in the temperatures range of 263–323 K. The expected decrease with increasing temperature is interrupted by a minimum near 283 K (Fig. 8), followed by apparently a second minimum near 316 K. The maximum around 303 K is in the same region as the change in the temperature coefficient seen in Fig. 3.

Similar behaviour has been observed in the temperature variation of T_1 for ^{14}N NQR in triethylenediamine which has a deep minimum ascribed to reorientation of the whole molecule about its threefold axis, followed at higher temperatures by an increase in the contribution from torsional oscillations of the whole molecule [18], and for ^{35}Cl T_1 in the disordered phase of *m*-chloronitrobenzene, ascribed to reorientation of the NO_2 group [12]. In both cases, the presence of a minimum or inflection in T_1 indicates the presence of magnetic dipolar relaxation.

The PETN phase I crystal structure is ordered at room temperature and stable up to close to the melting point near 416 K [6,7]. The PETN molecule sits on a fourfold inversion axis and the NO_3 group is planar, with ONO bond angles of 112.5°, 117.1° and 130.4°. The N–O bond lengths are 120 and 123 pm and the ONO bond angles to the CO_1 oxygen atom are 113° and 130°. Hindered rotation of the NO_2 group by 180° about the bond to the CO_1 oxygen atom will modulate the $^{14}N\ldots{}^{1}H$ dipolar coupling due to the transient reorientation of the interproton vector of the CH_2 group already discussed in the analysis of the ^1H NMR T_1 dispersion. If we neglect any contributions from quadrupole relaxation, the dipolar mechanism will be assumed to follow equations similar to (4)–(6) but appropriate to magnetic dipolar relaxation between unlike nuclei:

$$\frac{1}{T_{1_Q}} = C\left(\frac{\tau_c}{1+((\omega_Q-\omega_H)\tau_c)^2}+\frac{3\tau_c}{1+(\omega_Q\tau_c)^2}+\frac{6\tau_c}{1+((\omega_Q+\omega_H)\tau_c)^2}\right) \tag{10}$$

where

$$C = \frac{9}{160}\gamma_N^2\gamma_N^2\hbar^2\left(\frac{\mu_0}{4\pi}\right)^2\frac{\sin^2(2\alpha_{NH})}{r_{NH}^6} \tag{11}$$

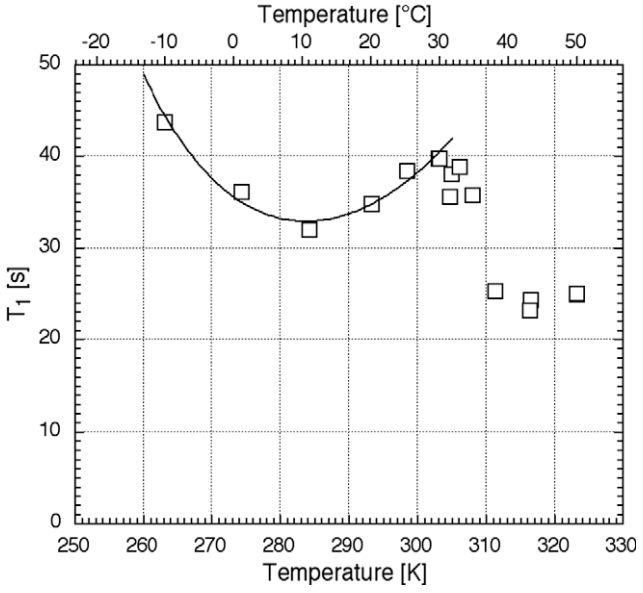

Fig. 8. Temperature dependence of T_1 for the ^{14}N NQR ν_+ line of PETN between 263 and 323 K.

and the correlation time τ_c is again given by Eq. (6). $2\alpha_{NH}$ is the mean transient angular change in the N...H vector due to the reorientation of the interproton vector of the CH_2 group, r_{NH} is the N...H internuclear distance, γ_N the ^{14}N gyromagnetic ratio and $\omega_Q = 2\pi\nu_Q$. Although Fig. 3 shows that ν_+ varies from about 893 to 889 kHz over the temperature range of the fit we have used the fixed value of $\nu_Q = \nu_+ = 890$ kHz as this temperature variation does not significantly alter the fit. We assume that $\omega_H = 2\pi\nu_H$ where ν_H here is $\nu_L = 25$ kHz, the ^1H NMR frequency the in local dipolar field. The parameters obtained from the fit are $C = 3.44\times10^4\ s^{-2}$, $\tau_0 = 5.45$ ps, $E_a = 24.5$ kJ mol^{-1} and $\tau_c = 0.18$ μs at the minimum near 284 K. The value of C corresponds to a value for $\sin^2(2\alpha_{NH})/r_{NH}^6$ of $2.06(4)\times10^{56}$. The value of τ_c is approximately 25 times shorter than the value predicted from the ^1H NMR dispersion measurements. The conclusion that the ^{14}N NQR correlation times are much shorter than those of ^1H NMR is attributed to the slow spin–lattice cross-coupling between the two spin systems [19].

Above about 305 K, T_1 begins to shorten again and there is some evidence for another minimum near 316 K. However, because of the risks entailed in going to higher temperatures for this large sample, we have insufficient results in this region to be certain about this second minimum. If it is real then the value of τ_c at this minimum would still be 0.18 μs but the lower value of T_1 of 23 s implies a larger value for C of 4.78×10^4 and hence a larger value of $\sin^2(2\alpha_{NH})/r_{NH}^6 = 2.87\times10^{56}$. Both α_{NH} and r_{NH} are likely to change, but assuming the value of the latter equals the mean X-ray value of 220 pm, the mean value of $2\alpha_{NH}$ increases by approximately 13.7° consistent with the increase in the torsional amplitude of the NO_2 group predicted by the reduction in the torsional frequency above 300 K. Despite the approximations made in the analysis the results of the NMR and NQR relaxation time measurements summarized in Table 3 are reasonably consistent with the proposed relaxation mechanism.

3.5. ^{17}O Quadrupole interactions

The third region of the proton T_1 dispersion between 1 and 10 MHz contains shallow but reproducible quadrupole dips, which are shown in more detail in Fig. 9, where the signal-to-noise ratio has been enhanced by application of a smoothing function in the form of a running average over 5 data points.

If the background variation is fitted by a power law term (Eq. (8)) which is then subtracted from the dispersion plot of Fig. 9, the quadrupole dip "spectrum" shown in the lower (solid line) plot is obtained. There is one broad quadrupole dip at a frequency of approximately 3.1 MHz and possibly three others at 4.2, 4.9 and 5.4 MHz, a region in which quadrupole dips from ^{17}O would be expected.

Such signals have been seen in other compounds, *viz* ammonium persulphate [20] and the success of the experiment attributed to short ^{17}O spin–lattice relaxation but long ^1H relaxation times. The same factor may account for their appearance in PETN. Two NQR frequencies are expected for this spin-5/2 nucleus, corresponding to the transitions ± 1/2 → ± 3/2 and ± 3/2 → ± 5/2. When the asymmetry parameter is non-zero the double quantum transition ± 1/2 → ± 5/2 is also possible. In PETN two such sets of NQR frequencies are expected, one for the NO_2 averaged over the hin-

Table 3
The results of the NMR and NQR relaxation time measurements.

Temperature	$2\alpha_{HH}$ [rads] (NMR)	$2\alpha_{NH}$ [rads] (NQR)	Ratio ($2\alpha_{HH}/2\alpha_{NH}$)
Below 310 K	0.066	0.019	3.68
Above 310 K	0.057	0.016	3.75
Ratio	1.15	1.18	

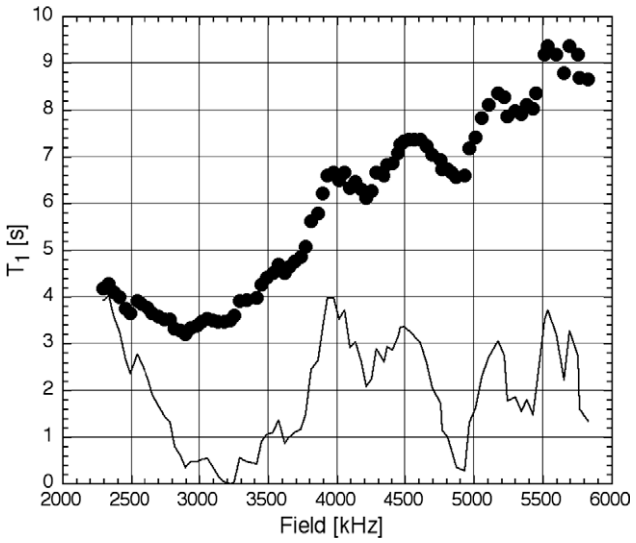

Fig. 9. The upper plot shows the data points for the ^{1}H T_1 dispersion measurements at 302 K between 2.3 and 5.8 MHz; two different sets of experiments have been averaged and enhanced by the application of a smoothing function (see text). The lower (solid line) plot is a quadrupole dip "spectrum" derived by subtraction of an estimate of the background variation from the dispersion data (the vertical scale does not apply to the lower plot since for this the scale is arbitrary).

dered rotation and the other for the CO oxygen which presumably is only marginally affected by this motion. For the former, the quadrupole parameters for an NO_2 group undergoing hindered rotation about an axis to a third atom can be estimated from published values of the quadrupole coupling constants and asymmetry parameters in nitrobenzene [21] at 77 K at which temperature all motion would be frozen. From a theoretical analysis, the maximum principal component of the electric field gradient (efg), q_{zz}, is found to lie in the molecular plane but perpendicular to the N–O bond with q_{xx} perpendicular to the molecular plane and a positive quadrupole coupling constant. A 180° rotation of the NO_2 group about the N–O_1 to the carbon atom will then rotate the efg tensor by 130.4° about the *x*-axis; averaging the two tensors over this motion and re-diagonalising gives an averaged quadrupole coupling constant of 4.977 MHz and asymmetry parameter of 0.141, corresponding to a rotation of 51° about the *x*-direction. The predicted NQR frequencies are then 0.762 and 1.487 MHz, where they would partly overlap the ^{14}N quadrupole dips. It appears that the observed spectrum must be assigned to the CO oxygen atom, its relaxation time reduced by the modulation of the ^{17}O....^{1}H dipole–dipole interactions due to the reorientation of the NO_2 group. A tentative assignment would be for the broad line near 3.1 MHz to correspond to the 1/2–3/2 transition and the higher frequency near 4.9 MHz to the 3/2–5/2 transition; additional weaker maxima may be due to Zeeman splitting of the ^{17}O quadrupole levels. If this assignment is correct, then the observed frequencies correspond to a ^{17}O quadrupole coupling constant of 17.5 MHz and an asymmetry parameter of 0.43. Alternatively, if the two ^{17}O frequencies are 3.10 and 5.40 MHz, the quadrupole coupling constant is calculated to be 18.4 MHz and asymmetry parameter 0.36, the most probable result lying between these two. Both values are large compared with the values observed in ice [22].

4. Conclusions

The results of combined ^{14}N NQR measurements and ^{1}H T_1 NMR dispersion between 1.8 kHz and 40 MHz in the explosive pentaerythritol tetranitrate (PETN) can be explained by a hindered rotation of the NO_2 group about the bond to the CO oxygen atom. The resulting transient change in the ^{14}N...^{1}H dipole–dipole interaction produces a step in the ^{1}H T_1 dispersion between 2 and 100 kHz characterised by a correlation time approximately 25 times longer than that of the reorientational jumps of the NO_2 group, attributed to slow spin–lattice cross-correlation between the ^{1}H and ^{14}N spin systems. The ^{14}N spin–lattice relaxation times appear to show an additional minimum near 316 K in the same region as the reduction in the NO_2 torsional frequency, explained by an increase in the torsional amplitude of the NO_2 group. The ^{1}H T_1 dispersion plots also contain information on the quadrupole resonance frequencies of the ^{14}N and possibly of the ^{17}O nuclei in this molecule, an added advantage of this NMR technique.

Acknowledgment

The authors thank the Defence Science and Technology Laboratory at Fort Halstead for support of this project.

References

[1] F. Noack, NMR field cycling: principles and applications, Progr. NMR Spectrosc. 18 (1986) 171–276.
[2] A.G. Redfield, Shuttling device for high-resolution measurements of relaxation and related phenomena in solution at low field, using a shared commercial 500 MHz NMR instrument, Magn. Reson. Chem. 41 (2003) 753–768.
[3] D. Plendl, M. Fujara, A.P. Privolov, F. Fujara, Energy efficient iron-based electronic field-cycling magnet, J. Magn. Reson. 198 (2009) 183–187.
[4] M. Blanz, T.J. Rayner, J.A.S. Smith, A fast field-cycling NMR/NQR spectrometer, Meas. Sci. Technol. 4 (1993) 48–59.
[5] R. Kimmich, F. Winter, W. Nusser, K.-H. Spohn, Interactions and fluctuations deduced from proton field-cycling spectroscopy of polypeptides, DNA, muscles and Algae, J. Magn. Reson. 68 (1986) 263–282.
[6] J. Trotter, Bond lengths and angles in penterythritol tetranitrate, Acta Cryst. 16 (1963) 698–699.
[7] H.H. Cady, A.C. Larsen, Pentaerythritol tetranitrate II: its crystal structure and transformation to PETN I; an algorithm for refinement of the crystal structure with poor data, Acta Cryst. B31 (1973) 1864–1869.
[8] E. Fukushima, S.B.W. Roeder, Experimental Pulse NMR: A Nuts and Bolts Approach, Addison-Wesley, Reading, MA, 1981.
[9] R.A. Marino, J.M. Klainer, Multiple spin echoes in pure quadrupole resonance, J. Chem. Phys. 67 (1977) 3388–3389.
[10] M.D. Rowe, King's College London, unpublished data.
[11] H. Chihara, N. Nakamura, Study of Molecular Motion by Nuclear Quadrupole Resonance and Relaxation Advance Nuclear Quadrupole Resonance, J.A.S. Smith (Ed.), vol. 4, Heyden, London, 1980, pp. 1-69.
[12] J. Schneider, C.A. Meriles, L.A.deO. Nunes, S.C. Perez, The dynamics of the NO_2 group in the solid phase of *m*-chloronitrobenzene studied by Raman spectroscopy and ^{35}Cl NQR, J. Mol. Struct. 447 (1998) 13–19.
[13] S.C. Perez, M. Krupski, R.L. Armstrong, A.H. Brunetti, An NQR study of the thermally activated motion of the nitro groups in 3-nitrobenzene sulphonyl chloride, J. Phys. Condens. Matter 6 (1994) 6019–6026.
[14] R.J.C. Brown, Temperature dependence of quadrupole resonance frequencies under constant pressure, J. Chem. Phys. 32 (1960) 116–118.
[15] B.H. Meier, F. Graf, R.R. Ernst, Structure and dynamics of intramolecular hydrogen bonds a solid-state NMR study, J. Chem. Phys. 76 (2) (1982) 767–774.
[16] D. Stephenson, J.A.S. Smith, Nitrogen-14 quadrupole relaxation spectroscopy, Proc. Roy. Soc. Lond. A416 (1988) 149–178.
[17] F. Winter, R. Kimmich, Spin–lattice relaxation of dipole nuclei (I = ½) coupled to quadrupole nuclei (S =1), Mol. Phys. 45 (1982) 33–49.
[18] S. Zussman, A. Alexander, Pure nuclear quadrupole resonance in triethylene diamine, J. Chem. Phys. 48 (1968) 3534–3539.
[19] D. Wolf, Spin-Temperature and Nuclear-Spin Relaxation in Matter: Basic Principles and Applications, Clarendon Press, Oxford, 1979.
[20] N.F. Peirson, J.A.S. Smith, D. Stephenson, ^{17}O quadrupole dips in ammonium persulphate, Z. Naturforsch. 49a (1994) 345–350.
[21] C.P. Cheng, T.L. Brown, Oxygen-17 nuclear quadrupole double resonance spectroscopy results for N–O P–O and S–O bonds, J. Am. Chem. Soc. 102 (1980) 6418–6421.
[22] Y. Margalit, M. Shporer, Some features of double-resonance detection of ^{17}O NQR in ice, J. Magn. Reson. 43 (1981) 112–121.